Spontaneous Bifurcation of Single Peaked Current Sheets by Chaotic Electron Scattering

Kuang-Wu Lee* and Jörg Büchner Max-Planck-Institut für Sonnensystemforschung, 37191 Katlenburg-Lindau, Germany (Dated: November 8, 2018)

It is shown that single-peaked collisionless current sheets in a Harris-type equilibrium spontaneously bifurcate as a result of chaotic scattering of electrons at fluctuating magnetic fields near the center of the sheet, as demonstrated by a 2D kinetic particle-in-cell simulation. For this effect to be simulated explicit particle advancing is necessary, since the details of the electron motion have to be resolved. Unlike previous investigations of triggering bifurcated current sheet (BCS) where initial perturbations or external pressure was applied the bifurcation is spontaneous if thermal noise is taken into account. A spontaneous current sheet bifurcation develops quicker than a tearing mode or other plasma instabilities. It is shown that in the course of the current sheet bifurcation the Helmholtz free energy decreases while the entropy increases, i.e. the new, bifurcated current sheet is in a more propable state than the single-peaked one.

PACS numbers: 05.70.-a, 05.70.Ce, 52.35.Ra:

The stability and possible unstable decay of current sheets play a central role in astrophyics as well as in the laboratory, e.g. for magnetic energy dissipation and reconnection [1]. For the investigations of current sheet stability often single-peaked current sheets are used, as the one derived by Harris [2].

The free energy of equilibria can cause a number plasma instabilities which spontaneously arise from thermal noise like the dissipative tearing mode instability in resistive [3] and collisionless plasmas [4]. In fusion plasmas spontaneous magnetic reconnection is found recently in the poloidal current sheet, which is an initial equilibria in the Reverse Field Pinch (RFP)[5]. Since the single-peaked current sheet equilibria is unstable and magnetic reconnection frequently takes place, the equilibria stability is an important issue for current sheet evolution.

Magnetosphere is a natural plasma laboratory for the evolution of current sheet equilibrium. Indeed, more recent detailed investigations of current sheets, has shown that current sheets frequently are bifurcated (BCS) instead of single-peaked [6] [7][8]. It was also found that these BCS are electron dominated, e.g. by statistical analyses of measurements onboard the CLUSTER spaccraft mission [9].

BCS were also found in numerical simulations. In magnetic reconnection plan BCS was interpreted, e.g., as a pair of slow mode shocks which develop in the reconnection outflow region [10][11]. However, BCS were also observed in minimum plasma inflow conditions, for which magnetic reconnection is not expected [12]. In the current direction, BCS formation without plasma inflow is discovered as a result of anomalous momentum transport due to pressure-gradient driven lower hybrid drift instability [13].

In the direction perpendicular to current drift, current sheet splitting similar to BCS is observed after the saturation of tearing mode instability [14]. Note that these authors used an implicit numerical scheme for advancing the particles for their 2D particle-in-cell (PIC) code simulations. In order to initialize the tearing mode instability quickly they also imposed perturbations to trigger instability growth.

Schindler and Hesse [15] performed a one-dimensional particle-in-cell (1D PIC) simulation with an initial boundary pressing. They concluded that a quasisteady boundary compression forces a single-peaked current sheet evolves toward BCS, as an equilibrium relaxation process but not due to plasma instability

We now have found that single-peaked collisionless current sheets might spontaneously bifurcate, without boundary compression or imposing tearing mode perturbation initially, as long as the electron thermal fluctuations are considered properly. We found that magnetic field fluctuations can initially start from thermal noise at the center of current. The magnetic field fluctuations may lead to chaotic scattering of the electrons out of the central (current peak) region of the sheet [16], reducing the electron current flow there and adding current flows away from the center of the sheet as already discussed for laminar current sheets [17].

To prove this hypothesis quantitatively we carried out 2D electromagnetic particle-in-cell code simulations to investigate the evolution of Harris current sheet equilibrium. An explicit numerical scheme (XOOPIC) was implemented since the details of the electron cyclotron trajectories have to be calculated properly. The fastest processes up to electron plasma time scales $\omega_{pe}^{-1} = \sqrt{\epsilon_o m_e/ne^2}$ is resolved. The chosen current sheet has a width $2\lambda = 1.15d_i$ which is slightly larger than the ion inertial length $d_i = c/\omega_{pi}$ to cover the full width of the ion dissipation region of the current sheet. The equilibrium magnetic field of a Harris sheet equilibrium is $B_y(x) = B_0 \tanh(x/\lambda) = \sqrt{4\mu k_B} T N_0 \tanh(x/\lambda)$, where k_B , $T = T_i = T_e$, B_0 and N_0 are the Boltzmann constant, ion/electron temperatures, asymptotic magnetic

^{*} lee@mps.mpg.de

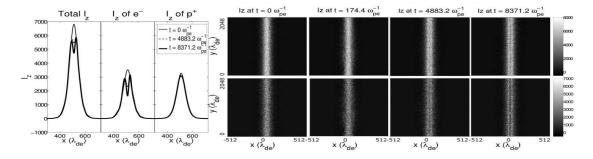


FIG. 1. The y-integrated current profiles (left panel) and current density at four different simulation times between t=0 and t=8371, 2 ω_{pe}^{-1} . The upper right panels show the total current and lower panels electron current densities.

field and number density at the center of the sheet, respectively. The ratio of electron plasma frequency to electron cyclotron frequency is $\omega_{pe}/\omega_{ce}=2.87$. The ion to electron mass ratio used is $m_i/m_e=180$, which is sufficient to separate the ion/electron motions. The grid size is of the Debye length $dx=dy=\lambda_{De}=(\varepsilon_0 T/Ne^2)^{1/2}$, which has sufficient spatial resolution of the detailed electron motion. The simulation domain in the direction perpendicular to the current sheet was $L_x=13.3d_i$ and in the current sheet direction $L_y=26.6d_i$. This choice of L_y allows a free development of the fastest growing tearing-type and other eigenmodes of the sheet (see, e.g., Eq.(23) in [18]). The boundary conditions for the particles and fields were chosen to be periodic in the y direction and conducting walls with particles reflection in the x direction

The time step used was $dt=0.0872~\omega_{pe}^{-1}=0.03~\omega_{ce}^{-1}$ to fulfill Courant condition and to resolve the detailed electron oscillation and cyclotron motions. Note that this time step is much smaller than the one used in implicit numerical schemes, where, e.g., in [14] $dt=0.1~\omega_{pi}^{-1}\approx 1.34~\omega_{pe}^{-1}\approx 0.5~\omega_{ce}^{-1}$ which does not track down the electron oscillation and cyclotron motion. The later is significant for magnetic scattering, which we will discuss soon. No initial perturbation was imposed as in [14]. Also, no boundary compression was imposed as in the 1D PIC simulation of BCS formation (see Fig.1 in [15]).

The left panels of Fig.1 show the y integrated total current density $I_z(x) = I_{z,e}(x) + I_{z,i}(x)$ and the individual contributions of electron $I_{z,e}$ and ion $I_{z,i}$: for the initial, single-peaked Harris-equilibrium currents by a thin solid line, for $t=4883.2~\omega_{pe}^{-1}$ by a dashed line and for $t=8371.2~\omega_{pe}^{-1}$ by a thick solid line. At the late stage $t=8371.2~\omega_{pe}^{-1}$ by a thick solid line. At the late stage $t=8371.2~\omega_{pe}^{-1}$ are integrated from each other. As one can see already in the middle panel of the left Fig.1 the reduction of $I_z(x)$ near the center of the current sheet is mainly due the spatial redistribution of the electron current. Since the ion current is not changing much before $t=8371.2~\omega_{pe}^{-1}$ the right panels of Fig.1 depict the evolution of the total current density distribution in the x,y plane with time in the upper row and the responsible for the current redistribution electron part in

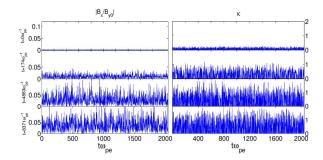


FIG. 2. Absolute values of the fluctuating $|B_x|$ magnetic fields at the center of the current sheet, normalized to the asymptotic magnetic field of the Harris equilibrium (left panel) and the thermal electron $\kappa(y)$ values at center of the current sheet (right panel) for the same four simulation times as in Figure 1, right panels.

the lower panels. While initially both the total and the electron currents are concentrated near the center of the sheet (first column in the right part of Fig.1), already at $t=4883.2~\omega_{pe}^{-1}=9.5~\omega_{ci}^{-1}=1.5\tau_{ci}$ a clear dip of the current density has developed around the center of the sheet. Here $\tau_{ci}=2\pi~\omega_{ci}^{-1}$ denotes a cyclotron period. Hence, the bifurcation takes place at the time scale of an ion cyclotron period. This result indicates that the ion-to-electron mass ratio $m_i/m_e=180$ used in the simulation the electron and ion dynamics are sufficiently well separated.

Note further that the bifurcation due to boundary pressing takes place only after $t \approx 400 \ \omega_{ci}^{-1}$ [15]. Their mass ratio is $m_i/m_e = 25$ and the bifurcation time in electron plasma period is $400 \ \omega_{ci}^{-1} \approx 4.4 \times 10^4 \ \omega_{pe}^{-1}$.

In order to understand this phenomenon one has to realize that plasmas are coarse-grained by their particles whose thermal motion lets currents and magnetic fields fluctuate at small scales. Hence, while the self-consistent magnetic field B_y of a Harris-equilibrium vanishes at the center of the sheet, fluctuating magnetic fields remain.

The left panel of Fig.2 shows $|B_x(x=0)|$, the absolute value of the normal field B_x component of the magnetic field at the center of the sheet, divided by the asymptotic Harris sheet field $B_{yo} = B_0$ for the same simulation times

as chosen for the right panels in Fig. 1. As one can see, $|B_x(x=0)|$ is finite most of the time unless the particles' thermal velocity is not taken into account as in the the uppermost column (t = 0). It is well known that particles transiting the center of current sheets can be chaotically scattered of the curvature of the magnetic field is comparable to the Larmor radii. According to Büchner and Zelenyi [16] the scattering is strongest, when the parameter $\kappa = \sqrt{R_{min}\rho_{max}}$ is unity, where R_{min} and rho_{max} are the minimum curvature of the magnetic field and and the maximum particle gyroradius at the current sheet center. The right panel of Fig.2 depicts the κ values for thermal electrons along the y direction for the same moments of time for which the $B_x(y)$ fields are shown in the left panel of this Figure and in the right panel of Fig.1. As one can see in the right panel of Fig.2 before t = $4883 \,\omega_{pe}^{-1} \,\kappa$ reaches unity only at a few positions, i.e. only at a few places the electrons are strongly scattered. After $t = 4883 \ \omega_{pe}^{-1}$ electrons are strongly scattered chaotically at many positions.

The consequences of this strong scattering can be described best by means of the action integral of the fast motion motion $I = \oint v_z dz$ [19]. For $\kappa < 1$ this action integral can be expressed in its normalized form as $I' = \left(\frac{\kappa^2 y'}{2k^2 - 1}\right) f_{A/B}(k)$, where k(y') is a function of y', the appropriately normalized y coordinate of the slowly moving guiding center and $f_{A/B}(k)$ are two different functions of complete elliptic integrals for k < 1and k > 1, respectively [16]. For $\kappa < 1$ the action integrals I' are adiabatically conserved, i.e. integrals of motion, as long as they stay away from the separatrix which is reached when $k \to 1$. For k < 1 such quasiadiabatic orbits cross the center of the current sheets while for k > 1 they will gyrate at some distance from the sheet center. Particles with $1 < I' < I'_{max} = 1.16$ are trapped on crossing the current sheet orbits k < 1. But in thin current sheets most particles will have I' < 1, which enables them to eventually reach a separatrix in the velocity space, i.e. change from the region k < 1to k > 1, at k = 1 changing from meandering across the sheet, drifting in the direction of the original sheet current to a gyration away from the current sheet center where they drift in the opposite direction, causing diamagnetic currents away from the sheet center [16]. While for $\kappa \ll 1$ particles the value of the quasi-integral of motion I' stays practically unchanged during the sepratrix encounter, for $\kappa \to l$ it can be essentially changed. If the obtained value of I' is very small only a small amount of kinetic energy is left in the perpendicular to the magnetic field velocity direction while most energy is in the slow drift motion. These particles contribute significantly to the built up of diamagnetic currents away from the sheet center. For small I' the asymptotic expressions for the elliptic integrals reveal $I' \approx 3/16\pi k_{tp}\kappa^6$, where k_{tp} correspond to the turning point of the drift motion in y' $(v_{y'}=0)$. From the condition for turning the drift in the y direction one obtains the position of the turning point by solving the equation $\kappa^2 y'_{tp} = 2k_{tp}^2 - 1$. Solving

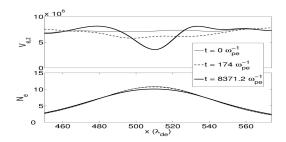


FIG. 3. Profiles of electron drift velocity $V_{e,z}$ (upper panel) and number density N_e (lower panel), both integrated along the y axis.

this equation for k_{tp} s and calculating the mean z-position for the turning point location one obtains a the distance $\Delta z \sqrt{\lambda \rho_{the}} (16\pi/3)^2 I'_{the}$ from the current sheet at which most of the particles drift in the dia-magnetic current direction. Here I'_{the} means the quasi-adiabatic invariant for typical thermal electrons, the bulk drift velocity of the electrons is much smaller and can be neglected. With the time being Δz will become the position of the maximum of the dia-magnetic flow of the electrons where the initial current profile is modified most by electron flows while the electron flow at the center of the current sheet is reduced. For the parameters used in the simulation one obtains $\Delta z \cong 27\lambda_{De}$. This theoretically predicted distance corresponds to the one found in simulation.

The Y integrated electron drift $V_{e,z}$ and density N_e profiles are show in Fig.3 for three moments of time. Note that such current profile was obtained by Hoshino et al. [7] from a statistical analysis of many current sheet encounters in the Earth's magnetotail. The electron number density does not change much in the course of the bifurcation, which happens, instead, in the electron drift velocity space. This is consistent with the finding that the current depletion at the center is caused mainly by the redistribution of the electrons by pitch-angle scattering in the velocity space when crossing the sepratrix between meandering (k < 1) and gyrating away from the sheet center (k > 1). Due to the mass ratio only the electrons undergo strong chaotic scattering thin Harristype current sheets. The new, bifurcated current sheet is again in equilibrium. In fact there is an infinite number of possible current sheet equilibria. A number of analytical [20] and non-analytical equilibrium solutions have been found which are more realistic for space current sheets than Harris sheets [21]. For a survey see, e.g., [22]. A current sheet bifurcated out of a single peaked Harris current sheet by the chaotic electron scattering is close to the equilibrium found by Camporeale and Lapenta [14], their case (b). Note that the BCS, naturally obtained via chaotic electron scattering, is more probable than the single peaked Harris sheet. This can be demonstrated by calculating the entropy of the system. For a plasma with a continuous particle distribution, it is appropriate to consider the relative Kullback-Leibler entropy which is always positive [23]. With respect to a reference distri-

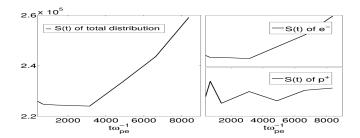


FIG. 4. Evolution of the total relative entropy (left panel) and of the electron (upper right panel) and ion entropies (lower right panel) separately.

bution q(v) at t = 0 it can be written as

$$S_{KL}(t) = \int_{-\infty}^{\infty} dv f(v, t) ln(\frac{f(v, t)}{q(v)|_{t=0}})$$

The relative entropy as a sum of the electron and ion contributions grows increases in the course of current sheet bifurcation. Looking at the electrons and ions separately one can see that the entropy of electrons is, indeed, steadily increasing after about $t=3800~\omega_{pe}^{-1}$ while the ion entropy oscillates (right columns of Fig.4). The stability of a steady state equilibrium can be analyzed by calculating the Helmholtz free energy F=U-T~S [24]. Here the U is the internal energy, a sum of the particles kinetic energy and the field energy, T is the temperature energy and S is the entropy. Less free energy F corresponds to a more stable equilibrium. In the course of the bifurcation, the internal energy U is conserved while T and S are increasing. Hence the bifurcated current sheet contains

less free energy. This is why it is more favored in nature than single-peaked equilibria like the Harris current sheet and it is more stable.

2D PIC simulations confirmed that an initially single peaked Harris equilibrium current sheet does spontaneously and quickly bifurcates a natural consequence of chaotic electron scattering due to their fluctuations at the center of the sheet. The bifurcation is faster than spontaneous plasma instabilities as of the tearing mode. The single peaked sheet bifurcates without initial perturbations or imposed external pressure. The bifurcated state is more favorable because electrons gaining after chaotic scattering at the sheet center toward small values of the quasi-adiabatic invariant of motion I' spends longer time in the cucumber phase of their motion away from the sheet center rather than meandering at the sheet center. Therefore it can be simulated only by numerical schemes that explicitly resolve the details of the electron motion. The spontaneous bifurcation of single peaked current sheets explains the frequent observation of bifurcated current sheets in quite situations without plasma inflows and reconnection as they are more stable than single peaked sheets. Their influence on plasma instabilities is stabilizing, delaying, lowering the growth rate, e.g., of the tearing mode instability.

ACKNOWLEDGMENTS

The authors are grateful to the Max-Planck Society for funding Turbulent transport and ion heating, reconnection and electron acceleration in solar and fusion plasmas Project No. MIF-IF-A-AERO8047.

- [1] J. Büchner, Space Sci. Rev. 122, 149 (2006).
- [2] E. G. Harris, Nuovo Cimento 23, 115 (1962).
- [3] H. P. Furth, J. Killeen, and M. N. Rosenbluth, Phys. Fluids 6, 459 (1963).
- [4] B. Coppi, G. Laval, and R. Pellat, Phys. Rev. Lett. 16, 1207 (1966).
- [5] M. Zuin, N. Vianello, M. Spolaore, V. Antoni, T. Bolzonella, R. Cavazzana, E. Martines, G. Serianni, and D. Terranova, Plasma Phys. Control Fusion 51, 035012 (2009).
- [6] V. A. Sergeev, D. G. Mitchell, C. T. Russell, and D. J. Williams, J. Geophys. Res. 98, 17,345 (1993).
- [7] M. Hoshino, A. Nishida, T. Mukai, Y. Saito, T. Yamamoto, and S. Kokubun, J. Geophys. Res. 101, 24775 (1996).
- [8] P. L. Israelevich, A. I. Ershkovich, and R. Oran, Planet. Space Sci. 55, 2261 (2007).
- [9] P. L. Israelevich, A. I. Ershkovich, and R. Oran, J. Geophys. Res. 113, A04215 (2007).
- [10] D. Shiota, H. Isobe, P. F. Chen, T. T. Yamamoto, T. Sakajiri, and K. Shibata, Astrophys. J. 634 (2005).
- [11] S. M. Thompson, M. G. Kivelson, M. El-Alaoui, A. Balogh, H. Réme, and L. M. Kistler, J. Geophys.

- Res. **111**, A03212 (2006).
- [12] C. L. Tang, L. Lu, Z. Y. Li, and Z. X. Liu, Chinese Phys. Lett. 23, 1054 (2006).
- [13] W. Daughton, G. Lapenta, and P. Ricci, Phys. Rev. Lett. 93, 105004 (2004).
- [14] E. Camporeale and G. Lapenta, J. Geophys. Res. 110, A07206 (2005).
- [15] K. Schindler and M. Hesse, Phys. Plasmas 15, 042902 (2008).
- [16] J. Büchner and L. M. Zelenyi, J. Geophys. Res. 94, 11821 (1989).
- [17] L. Zelenyi, H. Malova, and V. Popov, JETP Letters 78, 296 (2003), 10.1134/1.1625728.
- [18] M. Brittnacher, K. B. Quest, and H. Karimabadi, J. Geophys. Res. 100, 3551 (1995).
- [19] B. U. Ö. Sonnerup, J. Geophys. Res. **76**, 8211 (1971).
- [20] T. Neukirch, F. Wilson, and M. G. Harrison, Phys. Plasmas 16, 122102 (2009).
- [21] S. Cowley, Planet. Space Sci. 26, 1037 (1978).
- [22] K. Schindler and J. Birn, J. Geophys. Res. 107, A8, 1193 (2002).
- [23] S. Kullback and R. A. Leibler, Ann. Math. Statist. 22, 79 (1951).
- [24] J. R. Kan, J. Plasma Phys. **7**, 445 (1954).